Faraday Discussions

Cite this: *Faraday Discuss.*, 2019, **218**, 172

PAPER

Structural investigation of coal humic substances by selective isotopic exchange and high-resolution mass spectrometry†

Alexander Zherebker, *[ab] Irina V. Perminova, [b] Yury Kostyukevich,[ac] Alexey S. Kononikhin,[cd] Oleg Kharybin[a] and Eugene Nikolaev[a]

Received 6th January 2019, Accepted 25th January 2019
DOI: 10.1039/c9fd00002j

Here, we report the application of a selective liquid-phase hydrogen/deuterium exchange (HDX) coupled to ultra-high resolution FTICR MS for structural investigations of individual constituents of humic substances (HS) isolated from three coal samples of different geographical origin. Selectivity was achieved by conducting reactions in DCl or NaOD solutions for catalyzing HDX in aromatic ring and side-chain positions with enhanced C–H acidity, respectively. FTICR MS analysis showed a significant overlap of molecular compositions in the HS samples under study, with 2000 common formulae. Using HDX, we demonstrated that the determined common formulae are presented by different structural isomers. We found that aromatic compounds varied both in the substitution pattern and the number of aromatic protons. Depending on the sample, lignin components with the same molecular formulae were composed of coumaryl, coniferyl or sinapyl moieties. Enumeration of HDX series for the 800 most abundant compounds showed that the results of HDX agreed well with the model structures suggested for humic components occupying a van Krevelen plot. In addition, we explored chemical transformations, which could connect individual constituents of coal HS. These transformations included hydrolysis of a guaiacyl moiety and reduction of a catechol unit, which corresponds to the conversion of a coniferyl fragment into a coumaryl unit. The obtained results were supportive of the hypothesis of the reducing humification pathway suggested for lignin transformation in the environment. The conclusion was made that the molecular ensemble of coal HS is composed of individual constituents produced at different humification stages.

[a]*Skolkovo Institute of Science and Technology, Skolkovo, Moscow Region, 143025, Russia. E-mail: a.zherebker@skoltech.ru*

[b]*Department of Chemistry, Lomonosov Moscow State University, Leninskie Gory 1-3, Moscow, Russia*

[c]*Moscow Institute of Physics and Technology, Dolgoprudnyi, 141700 Moscow Region, Russia*

[d]*V.L. Talrose Institute for Energy Problems of Chemical Physics, Russian Academy of Science, Moscow, Russia*

† Electronic supplementary information (ESI) available: Additional information on the molecular compositions of coal CHM and a list of HDX results for the 800 most abundant compounds in CHM-Pow. See DOI: 10.1039/c9fd00002j

1. Introduction

Humic substances (HS) are the products of microbial and abiotic oxidation of remnants of living organisms. They are ubiquitous in the environment and constitute the major fraction of organic matter of caustobioliths, in particular of low grade coal (lignite and leonardite), peat, and oil shale.[1] Unlike petroleum, which consists mostly of hydrocarbons and aromatic heterocycles, coalified humic matter is enriched with oxygen-containing compounds carrying carboxylic and phenolic groups.[2] These compounds represent a complex mixture arranged into a supramolecular ensemble.[3] An analysis of different humification models enables the designation of various aromatic molecules with aliphatic side-chains and functional groups, and polyphenols with C–C and C–O–C ether bonds, as essential components of coal HS.[4] Aromatic constituents possess a pronounced biological activity.[5–7] It was shown that coal HS demonstrated the highest activity among HS from different sources.[8] In addition, the acidic character of coal HS is responsible for their metal binding properties, which are of particular importance for agricultural applications:[9] they can be used for plant nutrition in the form of water-soluble complexes with microelements.[10] At the same time, the application of coal humic materials is hindered by the extreme molecular heterogeneity of HS. Only high-resolution analytical techniques are capable of characterising their major structural moieties.[11]

NMR spectroscopy is the most powerful method for structural studies. In the case of HS, only partial structures can be identified due to substantial peak overlap.[12,13] The development of multidimensional NMR techniques enabled much deeper investigation of the aliphatic moieties of HS. Carboxylic rich alicyclic moieties (CRAM) were discovered.[14] Isotopic labeling extends NMR spectroscopy opportunities. The introduction of $^{13}CH_3$ groups in phenolic and carboxyl groups allowed Bell *et al.* to reveal the substitution pattern of aromatic rings and to suggest several possible structures of individual compounds in HS.[15] However, a higher resolution is required to investigate all constituents in complex organic mixtures. Thus, ultrahigh resolution FTICR mass spectrometry has become an indispensable tool for molecular exploration of HS.[16]

Due to its unprecedented high resolution power and mass accuracy, FTICR MS enables identification of thousands of molecules in complex mixtures.[17] The conventional approach is to plot FTICR MS data for HS in a van Krevelen diagram, which is a projection of molecular formulae on O/C and H/C atomic ratio coordinates.[18] Furthermore, van Krevelen plots can be binned into regions corresponding to typical molecular compositions of major HS precursors: lignins, flavonoids, tannins, carbohydrates, *etc.*[19,20] It performs classification tasks[21] but conveys only general information on the structure. In fact, the molecular composition may correspond to a number of different structural isomers, which cannot be resolved by FTICR MS.[22]

To avoid this limitation of FTICR MS, selective labeling of individual components of HS was introduced.[23] Each component undergoes a certain amount of chemical modifications according to its structure. This process is determined as a mass-shift from the parent ion in the mass-spectrum. H/D exchange (HDX) is the simplest technique of chemical labeling. Dissolution of an organic compound in D_2O results in a fast exchange of all labile protons with close to normal

distribution of peak intensities in the mass-spectrum.[24] HDX was applied for comparison of HS and their fractions.[25,26] Analysis of HDX series revealed a number of labile protons in the molecules observed in the FTICR mass-spectrum. The power of HDX mass spectrometry is discussed in detail in the corresponding review article.[27] Nevertheless, simple HDX lacks selectivity. Moreover, previously we demonstrated that due to the acceleration of chemical reactions in the charged microdroplets of electrospray, HDX with D_2O can result in additional exchanges of skeletal protons in the moieties with enhanced C–H acidity.[28] Recently, we developed a technique for selective deuteromethylation of carboxylic groups coupled to FTICR MS, which drastically reduces the ambiguity of HDX.[29] Its application to the fractions of HS from different sources (including coal) has shown the similarity of distributions of carboxyl-carrying constituents over van Krevelen diagrams in all fractions studied. The identified constituents were in accordance with the model structures of lignins, condensed tannins and carboxylic rich unsaturated oxygenated compounds. Still, this technique enables the exploration of functional groups, but not carbon skeleton structures.

In our previous work, we applied NaOD and DCl catalyzed exchange reactions[30] to synthetic humic-like substances to facilitate selective HDX of backbone protons in their individual constituents. This enabled elucidation of the exact structures of six products of oxidative condensation.[31] The objective of this study was to apply selective liquid-phase HDX coupled to FTICR MS to three HS samples from different varieties of lignite in order to identify the structural motifs of their common molecular constituents and to determine the exact structural differences of the determined isomers.

2. Materials and methods

2.1. Materials and reagents

Coal hymatomelanic acid (CHM) was isolated *via* exhaustive ethanol extraction in Soxhlet apparatus of freshly precipitated humic acids obtained by acidification of potassium humates produced from two leonardites (Powhumus, Germany and "Gumat-80", Irkutsk, Russia) and from a lignite deposit in Buryatia (Russia). The samples were designated CHM-Pow, CHM-Irk, and CHM-Gl, respectively. The solvents and other reagents used in this study were of analytical grade. Ethanol and methanol for HPLC (Lab-Scan) were used for elution and dissolution. High-purity distilled water was prepared using a Millipore Simplicity 185 water purifying system. Bond Elut PPL (Agilent Technologies) cartridges (100 mg, 3 mL) were used for isolation of labeled CHM samples.

2.2. Deuterium labeling of HS samples

HDX of CHM was performed according to the previously reported procedure.[31] A mixture of 5 mg of CHM with 300 μl of 4 M NaOD (or 16% DCl) in D_2O was heated at 120 °C for 40 hours in a sealed tube. After this step, the labeled material was desalted using solid-phase extraction on a Bond Elut PPL cartridge according to the protocol described by Dittmar *et al.*[32] Labeled CHM solutions were adjusted to pH 2 (in the case of DCl, the solvent was evaporated under vacuum followed by addition of 0.1 NaOH for CHM dissolution) and passed through the activated cartridge. To assure a back-exchange of labile protons, a washing step using

0.01 M HCl was repeated 3 times. The final solution was obtained *via* methanol elution. Native samples were redissolved and extracted following the same procedure. Each solution was analyzed using FTICR MS.

2.3. Fourier transform ion cyclotron resonance mass spectrometry

All experiments were performed on an FTICR MS Bruker Apex Ultra spectrometer with a harmonized cell[33] equipped with a 7 T superconducting magnet and an electrospray ion source (ESI). Prior to analysis, all HS samples were diluted with methanol to 100 mg L^{-1} and then injected into the ESI source using a microliter pump at a flow rate of 90 μL h^{-1} with a nebulizer gas pressure of 138 kPa and a drying gas pressure of 103 kPa. A source heater was kept at 200 °C to ensure rapid desolvation in the ESI droplets. Mass-spectra were first externally calibrated using a carboxylated polystyrene standard made in house.[34] Internal calibration was systematically performed using the residual peaks of fatty acids,[35] reaching accuracy values < 0.2 ppm. The spectra were acquired within a time domain of 4 megawords in ESI(−) and 300 scans were accumulated for each spectrum. The resolving power was 530 000 at $m/z = 400$. The formulae assignment was processed using the lab-made "Transhumus" software designed by A. Grigoriev, which is based on the total mass difference statistics algorithm.[36] All molecular formulas were detected as singly-charged negative ions. The generated formulas were validated by setting sensible chemical constraints (O/C ratio ≤ 1, H/C ratio ≤ 2, element counts (C ≤ 120, H ≤ 200, O ≤ 60, N ≤ 2) and mass accuracy window < 1 ppm). Sulfur and phosphorus containing formulae were excluded from consideration due to their low content.[37] The assigned CHNO formulas were further plotted into van Krevelen diagrams.[18] Based on the O/C and H/C atomic ratios and the aromaticity index (AI),[38] formulae were grouped into 8 compound classes: "saturated" (H/C ≥ 1.5, O/C ≤ 0.3), "aliphatics" (H/C ≥ 1.5, O/C > 0.3), low-oxidized unsaturated (H/C < 1.5, AI ≤ 0.5, O/C ≤ 0.5), highly-oxidized unsaturated (H/C < 1.5, AI ≤ 0.5, O/C > 0.5), low-oxidized aromatic (0.5 < AI ≤ 0.67, O/C ≤ 0.5), highly-oxidized aromatic (0.6 < AI ≤ 067, O/C > 0.5), low-oxidized condensed aromatic (AI > 0.67, O/C ≤ 0.5) and highly-oxidized condensed aromatic (AI > 0.67, O/C > 0.5). AI was calculated according to the following equation:[38]

$$\mathrm{AI} = \frac{1 + \mathrm{C} - \mathrm{O} - \mathrm{S} - 0.5\mathrm{N} - 0.5\mathrm{H}}{\mathrm{C} - \mathrm{O} - \mathrm{S} - \mathrm{N} - \mathrm{P}} \quad (1)$$

2.4. HDX data treatment

The data from the labeling experiments were processed following an algorithm that was described in our previous work.[31,39] It implies extraction of peaks related to HDX series of individual CHM constituents from the full mass spectrum. Those series are produced by peaks with m/z difference of 1.006277, which corresponds to the substitution of a proton with a deuteron. These HDX series were manually determined for the 800 most abundant peaks of CHM-Pow and some common formulae of all samples under study to identify the number of exchangeable skeletal protons in each parent ion, as shown in Fig. 2. Due to the extreme complexity of mass-spectra and limitations in resolution power, automatic

determination of HDX series was impossible. Accordingly, the number of analyzed peaks was limited to 800 for labor- and time-saving reasons: they were represented by peaks with S/N ratio > 10 and a relative magnitude > 1%.[40] If the parent ion could not be detected in the mass spectrum of the labeled CHM, its position was marked by a red mark and HDX series were determined relative to the monodeuterated ion. This prevented misinterpretation. The error constraint was set to 0.0005 m/z.

3. Results

3.1. Comparison of molecular composition of HS from the different coal varieties

The obtained results of FTICR MS and elemental analysis data are shown in Table 1. For all samples, we determined more than 3 thousand molecular compositions. The CHM-Gl lignite sample was characterized by the maximum content of nitrogen exceeding 3%. Both leonardite samples (CHM-Irk and CHM-Pow) contained 1.5% and 1% of N, respectively. In accordance with elemental analysis, the intensity contributions of CHON species decreased from 50% in the case of CHM-Gl to 20% in the case of CHM-Pow. The average values of the FTICR MS parameters listed in Table 1 also varied among the HS samples used in this study and agreed well with the data of elemental analysis. The value of the number-averaged aromaticity index (AI)[38] was lower for the leonardite samples (0.5) as compared to that for lignite (0.6). CHM-Pow and CHM-Irk were also characterized with relatively reduced structures with a number-averaged $O/C_n \approx 0.4$, while CHM-Gl contained ~50% of oxygen by mass and $O/C_n = 0.5$.

To compare the HS samples from different coal varieties on a molecular level, we plotted all of their determined molecular formulae into van Krevelen diagrams (Fig. 1B–D). The latter were further binned into specific areas with respect to the value of aromaticity indexes and of atomic ratios, as described in the Materials and methods section. The intensity-weighted histogram of compound classes is presented in Fig. 1A. The HS samples used in this study possessed quite similar molecular distributions over van Krevelen diagrams. The most pronounced difference between the samples was the relative depletion with saturated compounds along with the higher content of oxidized condensed compounds with AI > 0.67 in CHM-Gl as compared to both CHM-Irk and CHM-Pow samples. At the same time, for all samples, the major components were attributed to compounds with AI > 0.5 and O/C < 0.5. Another common feature of the coal HS samples was the high contribution of low-oxidized unsaturated compounds with atomic ratios H/C < 1.5 and O/C < 0.5. These compounds are usually referred to as polyphenols and lignin, in particular,[19,20] which is considered to be the major precursor for coal humic substances.[41] The obtained results were also in agreement with our previous findings on the comparison of two HS samples isolated from different lignites, which were characterized by the higher contribution of oxidized species as compared to leonardite HS.[42]

The HS sample similarity is clearly visualized in a Venn diagram (Fig. S1†) presenting molecular composition overlap. We found that the three samples studied possessed almost 2000 common formulas (present in all three samples) and 2176 shared formulas (present in two samples). From all common formulae, 669, 765 and 508 could be attributed to lignin, aromatic and condensed

Table 1 The values of the FTICR MS average parameters and elemental compositions of the HS samples used in this study

	FTICR MS data									Elemental analysis			
Sample	Total formulae	CHO	CHON	CHO, % intensity	CHNO, % intensity	M_n[a]	Al_n[a]	O/C_n[a]	H/C_n[a]	C, %	H, %	O, %	N, %
CHM-Gl	3658	1616	2042	49.51	50.49	511.22	0.61	0.50	0.67	42.76	2.92	50.98	3.34
CHM-Irk	5443	3210	2233	69.87	30.13	493.19	0.55	0.43	0.80	55.73	3.58	39.19	1.5
CHM-Pow	3668	2386	1282	79.83	20.17	462.73	0.53	0.42	0.84	50.07	2.17	46.75	1.01

[a] n stands for the number-average values calculated according to the following equation: $X_n = \frac{\sum X_i I_i}{\sum I_i}$, where X = M, AI, O/C or H/C, and I = peak intensity.

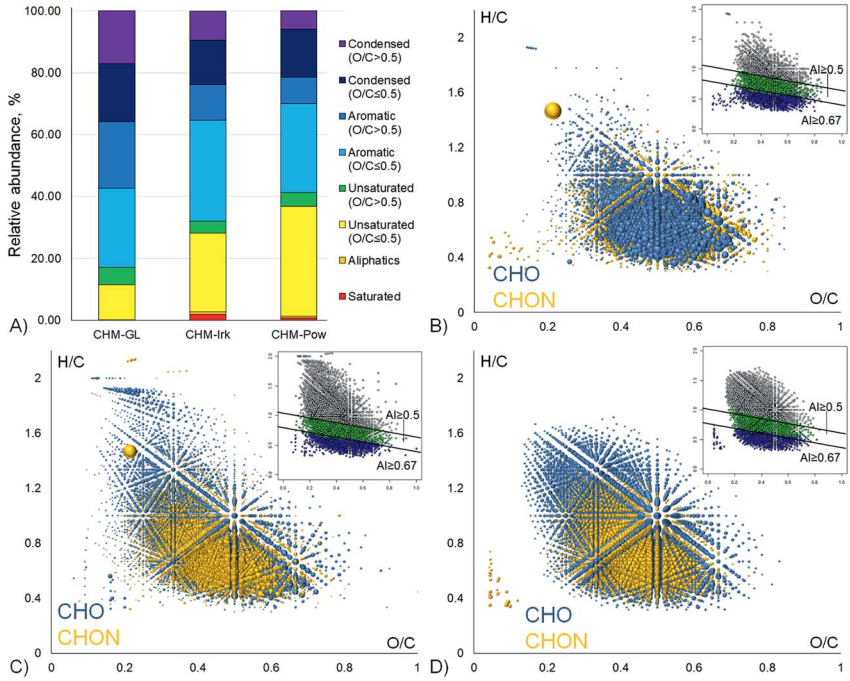

Fig. 1 Characteristics of molecular composition of the three coal HS under study: (A) the relative contribution of different molecular classes based on aromaticity index and O/C ratio; (B–D) van Krevelen diagrams for CHM-Gl, CHM-Irk, and CHM-Pow, respectively. The insets show the AI threshold for all samples: AI ≥ 0.67 (blue), 0.5 ≤ AI < 0.67 (green) and AI < 0.5 (gray).

compounds, respectively. This highlights the importance of polyphenols in the formation of coal organic matter.

The discovered substantial similarity of the molecular composition of the HS samples under study may lead to a wrong conclusion about the similarity of their origin and structural match of major components. In fact, a possible source of organic carbon for coal formation is terrestrial plant biomass, which underwent intensive transformations.[43] It has been reported that the coal originating from East Siberia and represented by CHM-Irk and CHM-Gl was formed during the Cretaceous period,[44] while coal from the German mine is significantly younger, originating from the Middle Miocene.[45] These geological periods were characterized by different vegetation and, therefore, different biomolecular precursors for coal formation. This should have resulted in the structural variance of the major components of the samples under study behind the common molecular compositions.

3.2. H/D exchange of skeletal protons with basic or acidic catalysis

For comparison of the coal HS used in this study on the structural level, we performed acid/base catalyzed H/D exchange of aromatic protons. A reaction scheme is presented in Fig. 2. In DCl, HDX proceeds exclusively *via* electrophilic substitution in the aromatic ring.[30] Adverse HDX of side-chain protons occurs

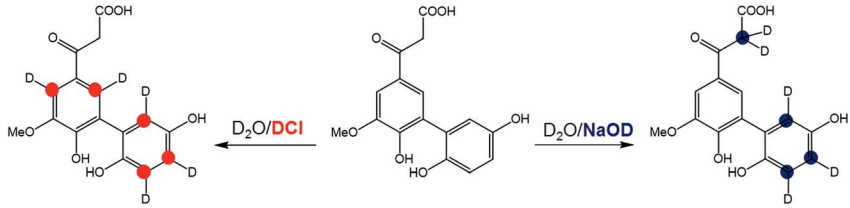

Fig. 2 Scheme of HDX, illustrating reaction regioselectivity under basic and acidic catalysis.

only under supercritical conditions, in which the D_2O/DCl mixture behaves as a super-acid.[46] In the case of NaOD, both aromatic and side-chain protons undergo HDX. In the aromatic ring, HDX is facilitated by keto–enol tautomerism of the phenolic group. So, only protons in *ortho*- and *para*-positions to the phenolic group undergo HDX. Side-chain protons undergo HDX in molecular sites with extended C–H acidity, such as benzylic and α-CH_n moieties.[30] Another advantage of the chosen HDX techniques is the low impact of reagents on the sample integrity. Unlike hydroiodic acid, DCl isn't able to cleave ether bonds at temperatures below 200 °C.[46] Also, a lack of oxidation and condensation processes in NaOD without continuous air flow was shown in our previous paper on the HDX of model humic compounds.[28]

Due to the high analytical capabilities of FTICR MS, parent and deuterated ions were resolved in mass-spectra. Using a custom R-script, we first extracted peaks, which may compose HDX series of the parent ions with nominal mass shift $\Delta m = 1.00628$ (for singly charged ions) as is schematically shown in Fig. 3 on the example of a neutral molecule $C_{19}H_{17}O_8$ identified in the CHM-Pow sample. Furthermore, we manually selected peaks with binomial distribution, which is a well-fitted approximation for HDX.[47] It is noteworthy that incomplete HDX would significantly confuse the data interpretation. Previously, we applied ^2H NMR spectroscopy and FTICR MS to evaluate regioselectivity and completeness of HDX reaction on the model humic and lignin monomers.[28] The chosen HDX technique facilitated a high deuteration degree, which resulted in the absence of the parent ion in the mass-spectrum of the labeled material and enabled determination of all exchangeable protons in molecules. Therefore catalytic HDX provides a high degree of deuteration, which combined with regioselectivity allowed us to reliably attribute exchangeable protons to the particular structural fragments of individual compounds.[31]

The determined lengths of HDX series obtained under acidic or basic conditions for 6 common formulae are presented in Table 2. Evaluation of the data enabled specification of the differences between the samples under study. We found that compounds with common molecular compositions possessed different amounts of specific exchangeable protons. It was necessary to perform both acidic and basic catalysis to explore structural differences in more detail. For example, for molecular composition $C_{17}H_{10}O_7$, we observed four HDX in NaOD for all samples. However, for the same composition in DCl, CHM-Pow, CHM-Irk and CHM-Gl possessed 5, 6, and 4 exchangeable protons, respectively. This indicates the presence of different isomers comprising CHM samples.

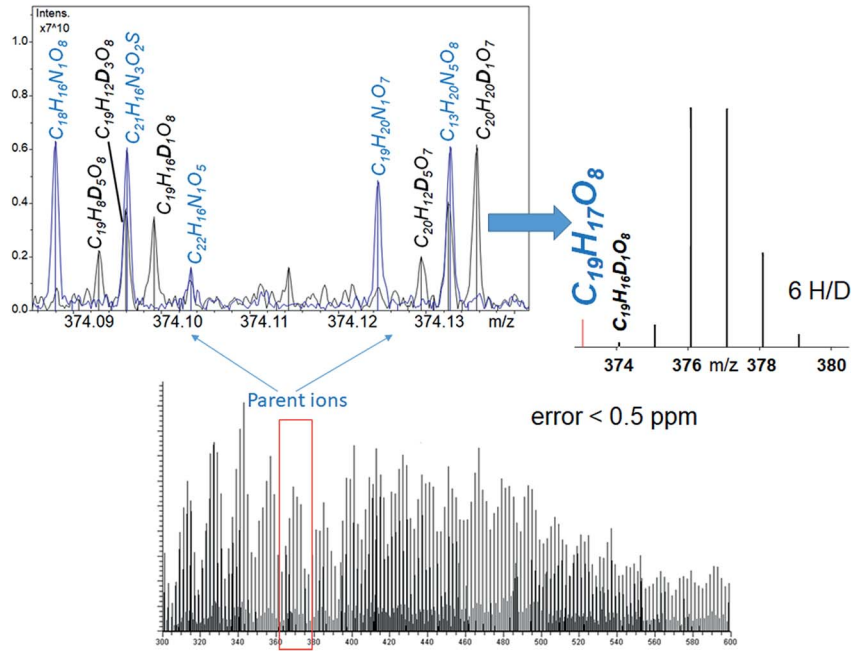

Fig. 3 FTICR mass-spectrum of D-labeled CHM-Pow with a magnified fragment at the nominal $m/z = 374$. Residual parent and deuterated ions are designated in blue and black colors, respectively. The inset on the right shows the mathematically extracted mass-spectrum fragment for determining the HDX series for $C_{19}H_{18}O_8$ molecular composition.

The regioselectivity of HDX and knowledge of the major humification pathways allowed us to suggest which structural motifs represent the differences in the number of exchanges. Given that under acidic conditions, only aromatic protons undergo HDX, the length of HDX is equal to the degree of aromatic rings substitution. This is particularly important for the lignin components of the coal HS under study, which are essentially composed of three model phenylpropanoic units: *p*-coumaryl, coniferyl and sinapyl moieties. They differ by the number of methoxyl substituents in aromatic ring as is shown in Fig. 4A.

The molecular formulae $C_{17}H_{20}O_7$ and $C_{16}H_{16}O_7$ are characterized by lignin-like compositions and the double bond equivalent (DBE) 9 and 8, respectively. We detected these molecules in negative ESI mode, so they likely contain carboxylic

Table 2 The number of exchangeable protons under acidic or basic (in parentheses) conditions determined for six common components of the coal HS samples under study

Formula	DBE	CHM-Pow	CHM-Irk	CHM-Gl
$C_{16}H_{16}O_7$	9	4(5)	3(3)	2(3)
$C_{17}H_{20}O_7$	8	4(5)	3(3)	1(3)
$C_{17}H_{10}O_7$	13	5(4)	6(4)	4 (4)
$C_{20}H_{14}O_6$	14	5(5)	4(1)	2(3)
$C_{14}H_{10}O_9$	10	0(0)	4(4)	3(3)
$C_{16}H_{10}O_{10}$	12	1(1)	4(4)	4(6)

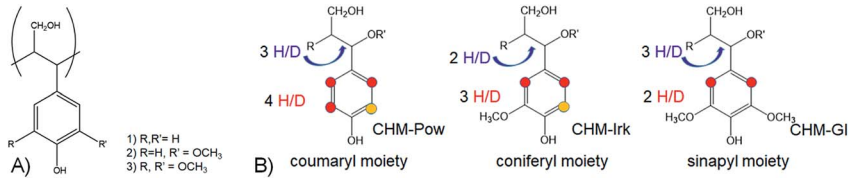

Fig. 4 A) Aromatic moieties of *p*-coumaryl (1), coniferyl (2) and sinapyl (3) alcohols; (B) phenylpropanoic fragments determined in isomers of $C_{16}H_{16}O_7$ by HDX of three samples of coal HS used in this study. The red, blue and orange circles correspond to protons subjected to HDX in DCl, NaOD and in both cases, respectively.

groups,[48] which facilitate ionization in the negative mode. This might be indicative of the presence of one aromatic ring in both $C_{17}H_{20}O_7$ and $C_{16}H_{16}O_7$. In this case, the length of HDX series under acidic conditions specifies the structure and origin of lignin compounds in the coal HS samples. For CHM-Pow, CHM-Irk, and CHM-Gl, we obtained four, three, and two HDX for $C_{16}H_{16}O_7$, which are attributed to *p*-coumaryl, coniferyl and sinapyl moieties, respectively, represented in Fig. 4B. Similar results were obtained for $C_{17}H_{20}O_7$, only in the case of the CHM-Gl sample, we observed one exchange instead of two. This could be explained by the formation of a five-membered dihydrofuran cycle between the vacant *ortho*-position in the aromatic ring and side-chain, which is typical for lignin.[49]

Application of HDX under basic conditions enables the comparison of side-chain structures for the common molecular compositions identified in the coal HS samples under study. Based on acidic HDX, we proposed the presence of *p*-coumaryl moieties for $C_{17}H_{20}O_7$ and $C_{16}H_{16}O_7$ molecules in the case of CHM-Pow. Under basic conditions, we observed 5 exchanges for these molecules. Two of the five exchanges could be attributed to C–H in *ortho*-positions to the phenolic group, which undergo HDX in alkaline solutions. Therefore, three of the five exchanges belong to the side-chain (Fig. 4B). In the case of CHM-Gl, all three exchanges (Table 2) belong to the side-chain, since the presence of methoxyl-groups prevents HDX in the aromatic ring. In the case of CHM-Irk, we observed 3 exchanges under basic conditions for $C_{16}H_{16}O_7$ and $C_{17}H_{20}O_7$. Based on acidic HDX, coniferyl moieties can be proposed for these molecules: they possess C–H protons at an *ortho*-position to the phenolic group, which are exchangeable in NaOD. Therefore, we suggest that in the case of CHM-Irk, both $C_{16}H_{16}O_7$ and $C_{17}H_{20}O_7$ possess 2 exchangeable protons in the side-chain (Fig. 4B).

Consideration of HDX results for low-oxidized aromatic compounds also reveals structural differences in the common components of the three coal HS samples under study. It can be suggested that these aromatic compounds can be attributed to tannins – the major HS precursors, which undergo oxidative condensation in nature.[50] Their aromatic structures have no side-chains and, hence, all HDX are taking place out in aromatic rings. For $C_{17}H_{10}O_7$, we observed 5, 6 and 4 exchanges in DCl for CHM-Pow, CHM-Irk, and CHM-Gl, respectively. The number of exchanges indicates the different degree of aromatic ring substitution. For $C_{17}H_{10}O_7$ in CHM-Pow, we may suggest a flavonoid-like structure with 5 non-substituted aromatic protons subjected to acidic HDX (Fig. 5A). Moreover, in NaOD we observed 4 exchanges for $C_{17}H_{10}O_7$. Proton 2 (Fig. 5A) is in a *meta*-position to the phenolic group, which explains the absence of HDX in

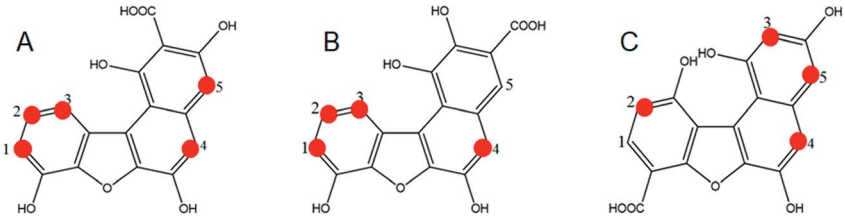

Fig. 5 Flavonoid-like structures proposed for low-oxidized aromatic compounds in coal hymatomelanic acids as revealed by HDX FTICR MS: (A) CHM-Pow, (B and C) CHM-Gl. The numbers indicate C–H bonds subjected to HDX. The red circles designate protons subjected to HDX in DCl.

NaOD. Collectively, HDX under acidic and basic conditions supports the structure depicted in Fig. 5A.

Variation in the order and position of the substituents in the aromatic ring affects the reactivity of the aromatic ring. For $C_{17}H_{10}O_7$ in CHM-Gl, we observed 4 exchanges in DCl. In this case, we suggested two possible structures depicted in Fig. 5B and C. The carboxylic substituent prevents electrophilic substitution and acidic HDX in positions 5 and 1 in the middle and right structures, respectively. In NaOD, we observed 4 HDX, which is in accordance with both suggested structures. The obtained results indicate that aromatic flavonoid-like components of coal HS may vary in substituent positions.

3.3. Structural motifs of different constituents of coal HS

The determination of HDX series for a number of ions determined in the coal HS samples under study enables comparison of different constituents in terms of their reactivity. Also, the obtained information may be used for attribution of molecular compositions to the particular classes of organic compound based on their projection in the van Krevelen diagram.[51] For this purpose, HDX series were determined for the 800 most abundant ions in the FTICR mass-spectrum of CHM-Pow (Table S1†). The results were plotted in a van Krevelen diagram with color designation of HDX series length for both DCl and NaOD (Fig. 6). It is seen that

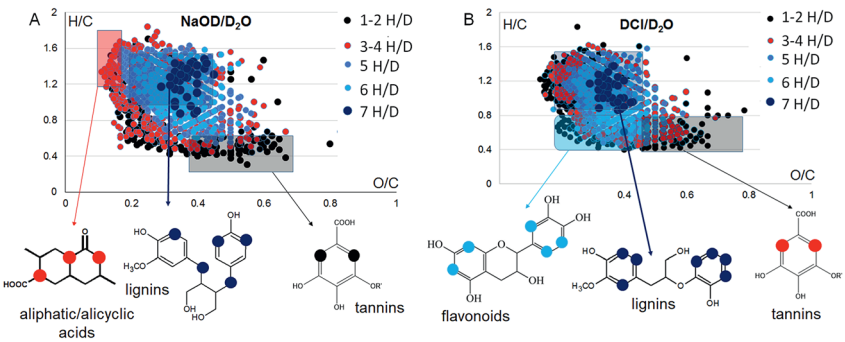

Fig. 6 Color-coded van Krevelen diagram for the 800 most abundant compounds in CHM-Pow with HDX series lengths obtained in (A) NaOD and (B) DCl, as well as model structures.

different components were characterized by different HDX lengths. In particular, the low-oxidized unsaturated components gave rise to the highest amount of exchangeable protons in both DCl and NaOD. Aliphatic compounds demonstrated HDX only in NaOD, while aromatic compounds underwent HDX in both DCl and NaOD. The obtained results are in agreement with the model structures of lignin, flavonoids, tannins and aliphatic/alicyclic carboxylic acids constituting HS.[52] So, oxidized aromatic compounds with H/C < 0.6 and O/C > 0.5 were characterized by a minimum amount of exchangeable protons (1-2 HDX). This agrees well with a gallic acid core proposed for tannins.[53] Low-oxidized aromatic compounds with H/C < 0.8 and O/C < 0.5 possessed up to 6 exchangeable protons in DCl and up to 4 in NaOD. These results are in good agreement with the model flavonoid-like structures shown in Fig. 6B. Low-oxidized unsaturated compounds with H/C > 1.2 and O/C < 0.2 possessed 3–4 exchangeable protons only in NaOD (Fig. 6A). Since HDX occurs in C–H bonds with increased acidity,[54,55] we assign these compounds to the alicyclic carboxylic acids, which undergo HDX in α-positions. The presence of alicyclic carboxyls was suggested previously using gradient fractionation of coal HS[56] and using NMR spectroscopy of pyrogenic soil HS.[57]

Polyphenolic compounds with O/C < 0.5 are of particular interest for structural determination due to their key role in HS biological activity.[8,58] In Fig. 6A, we see that the number of exchanges in NaOD increased with O/C from 5 to 7. An increase in O/C ratio could be accounted for by the presence of acceptor groups in the side-chain of molecules[29] and for hydroxylation of aromatic rings, which consequently creates new positions subjected to HDX. In typical lignin β-O-4 structures, there is a lack of non-substituted side-chain protons for HDX.[49] At the same time, phenolic fragments of phenylpropanoic units could undergo only two exchanges in NaOD as discussed above. Therefore, we suggest dibenzyl-butyrolactol-like (or dibenzyl-butyrolactone-like) structures,[59] as shown in Fig. 7, with a number of benzylic protons that are easily subjected to HDX due to enhanced C–H acidity.

In DCl, we observed a similar trend with the extension of HDX series lengths from 3 to 7 followed by DBE and O/C ratio increases (Fig. 6B). According to our previous results, these compounds are composed mostly of unconjugated carboxylic acids.[56] The absence of carboxylic groups in the aromatic ring

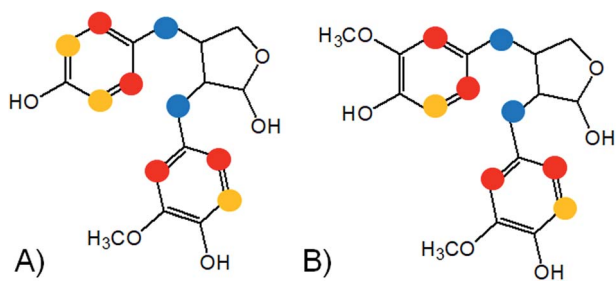

Fig. 7 Model dibenzyl-butyrolactol-like compounds suggested for (A) $C_{19}H_{22}O_5$ and (B) $C_{20}H_{24}O_6$ molecular compositions. The red, blue and orange circles correspond to protons subjected to HDX in DCl, NaOD, and in both cases, respectively.

results in high reactivity in electrophilic substitution, which leads to the efficient HDX.[30] Given that the amount of acidic HDX indicates the degree of aromatic ring substitution, we may compare structures of the different constituents of the coal HS samples under study. For example, $C_{19}H_{22}O_5$ and $C_{20}H_{24}O_6$ possessed 7 and 6 exchangeable protons under acidic conditions, respectively. The first molecule is likely to be composed of *p*-coumaryl and coniferyl moieties (Fig. 7A), while the second one includes 2 coniferyl fragments (Fig. 7B).

3.4. Unveiling lignin humification processes using HDX FTICR MS

Considering the structures of lignin-like polyphenols, we could explain an extension of the HDX series in NaOD along with an increase in the O/C ratio by incorporation of acceptor groups and oxidation processes. At the same time, the number of exchangeable protons correlated with the value of DBE, in particular, for the DCl catalyzed reaction. The observed trends could be related to chemical transformations, which occur during lignin humification. It was shown that in addition to oxidation and condensation processes, lignin humification is accompanied by hydrolysis of ether bonds.[41,60] In the case of coniferyl and sinapyl moieties, hydrolysis leads to the generation of a new phenolic group and consequently to an increase in O/C ratio, and to activation of aromatic protons for HDX under basic conditions. It is shown in Fig. 8A on the example of transformation of a guaiacyl unit into a coniferyl fragment. Hydrolysis of methyl ether results in the formation of a catechol moiety with an increase in the O/C ratio and DBE value due to elimination of the methyl group. Catechol undergoes additional HDX in NaOD in the *ortho*- and *para*-position to the new phenolic group. The further loss of a phenolic group (Fig. 8B) adds new aromatic protons for HDX in DCl. For example, according to HDX results, a compound with molecular formula $C_{20}H_{28}O_8$ in CHM-Pow possesses six aromatic protons, which corresponds to two coniferyl moieties. Its OCH_2 homologue – $C_{19}H_{26}O_7$ – possesses seven exchangeable aromatic protons, which could correspond to formation of a coumaryl moiety due to methyl ether hydrolysis. Therefore, application of selective HDX enables identification of different phenylpropanoic units within the same coal HS sample and determination of their chemical connectivity reflected in the general humification pathways.

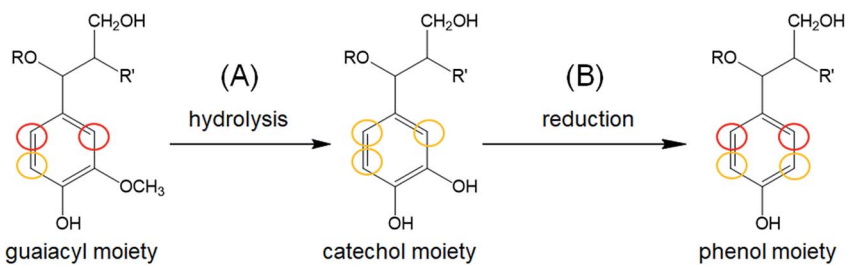

Fig. 8 General scheme of reducing lignin humification pathway: (A) hydrolysis of methyl ether, and (B) reduction of phenolic group.[60] The red and orange circles designate exchangeable protons in DCl, and in both DCl and NaOD, respectively.

4. Conclusions

The application of HDX enabled enumeration of specific exchangeable protons in the individual components of the three coal HS samples used in this study. Due to the regioselectivity of HDX achieved through liquid-phase catalysis, only sites with enhanced C–H acidity and aromatic protons underwent labeling in NaOD and DCl, respectively. According to the FTICR MS molecular profiles, the three samples under study contained more than 2000 common formulae. The clear differences in their structures were revealed using HDX. Under the same conditions, the so-called common components possessed different amounts of exchangeable protons. We suggested that aromatic constituents varied by the positioning of and by the number of aromatic protons. The degree of aromatic ring substitution, which was observed in DCl, indicated coniferyl, coumaryl and sinapyl moieties as composing lignin components of coal HS. The combination of HDX in DCl and NaOD enabled suggestion of the phenolic group positions in low-oxidized aromatic compounds. The generalization of the obtained data as a distribution of exchangeable protons in the van Krevelen diagram plotted for the 800 most abundant ions determined in FTICR mass-spectrum of the leonardite HS showed that HDX results agree well with the model structures of lignin, tannins, flavonoids and alicyclic carboxylic acids. In addition, HDX enabled exploration of the chemical transformations, which could connect individual lignin constituents of coal HS. Transformations included hydrolysis of the guaiacyl moiety followed by reduction of the catechol unit, resulting in the loss of a phenolic group in the aromatic ring. This transformation corresponded to the reducing humification pathway suggested for lignin in the environment. Hence, the molecular ensemble of coal HS is composed of individual constituents produced at different humification stages, which can be used as an evolution parameter of coal humic matter. The obtained information can be used for fine fractionation and isolation of organic components with the known structures from coal. This can be of great use for the non-fuel chemical industry by enabling production of new chemicals and materials from coal.

Conflicts of interest

There are no conflicts to declare.

Acknowledgements

This work was supported by Russian Science Foundation grant no. 18-79-10127 (FTICR MS and HDX studies). The isolation of coal hymatomelanic acids and their primary characteristics were conducted under support of Russian Foundation for Basic Research grant no. 16-04-01753. AZ and EN acknowledge support from the European's Horizon 2020 Research and Innovation Program under grant agreement No. 731077.

References

1 R. S. Swift. Organic Matter Characterization, in *Methods of soil analysis. Part 3. Chemical methods*, ed. D. L. Sparks, A. L. Page, P. A. Helmke, R. H. Loeppert,

P. N. Soltanpour, M. A. Tabatabai and C. T. Johnson, SSSA Book Series 5, SSSA, Madison, WI, 1996, p. 1036.

2 A. Nebbioso and A. Piccolo, Basis of a Humeomics Science: Chemical Fractionation and Molecular Characterization of Humic Biosuprastructures, *Biomacromolecules*, 2011, **12**(4), 1187–1199.

3 A. Piccolo, The Supramolecular Structure of Humic Substances, *Soil Sci.*, 2001, **166**(11), 810–832.

4 S. E. Cabaniss, G. Madey, L. Leff, P. A. Maurice and R. Wetzel, A Stochastic Model for the Synthesis and Degradation of Natural Organic Matter Part II: Molecular Property Distributions, *Biogeochemistry*, 2007, **86**(3), 269–286.

5 N. A. Kulikova, E. V. Stepanova and O. V. Koroleva, Mitigating Activity of Humic Substances: Direct Influence on Biota, in *Use of humic substances to remediate polluted environments: from theory to practice; Springer*, 2005, pp. 285–309.

6 A. Steinbüchel and R. H. Marchessault. *Biopolymers for Medical and Pharmaceutical Applications*, Wiley-VCH, John Wiley, 2005.

7 R. Klöcking and B. Helbig, Medical Aspects and Applications of Humic Substances, *Biopolymers For Medical & Pharmaceutical Application*, 2005, 3–16.

8 Y. V. Zhernov, S. Kremb, M. Helfer, M. Schindler, M. Harir, C. Mueller, N. Hertkorn, N. P. Avvakumova, A. I. Konstantinov, R. Brack-Werner, *et al.*, *Su*pramolecular Combinations of Humic Polyanions as Potent Microbicides with Polymodal Anti-HIV-Activities, *New J. Chem.*, 2016, **41**(1), 212–224.

9 M. Villén, J. J. Lucena, M. C. Cartagena, R. Bravo, J. García-Mina and M. I. M. De La Hinojosa, Comparison of Two Analytical Methods for the Evaluation of the Complexed Metal in Fertilizers and the Complexing Capacity of Complexing Agents, *J. Agric. Food Chem.*, 2007, **55**(14), 5746–5753.

10 K. Kovács, V. Czech, F. Fodor, A. Solti, J. J. Lucena, S. Santos-Rosell and L. Hernández-Apaolaza, Characterization of Fe-Leonardite Complexes as Novel Natural Iron Fertilizers, *J. Agric. Food Chem.*, 2013, **61**(50), 12200–12210.

11 R. Spaccini and A. Piccolo, Molecular Characterization of Compost at Increasing Stages of Maturity. 1. Chemical Fractionation and Infrared Spectroscopy, *J. Agric. Food Chem.*, 2007, **55**(6), 2293–2302.

12 N. Hertkorn and A. Kettrup, Molecular Level Structural Analysis of Natural Organic Matter and of Humic Substances by Multinuclear and Higher Dimensional NMR Spectroscopy, in *Use of Humic Substances to Remediate Polluted Environments: From Theory to Practice*, Springer-Verlag, Berlin, 2005, pp. 391–435.

13 I. V. Perminova, E. A. Shirshin, A. I. Konstantinov, A. Zherebker, V. A. Lebedev, I. V. Dubinenkov, N. A. Kulikova, E. N. Nikolaev, E. Bulygina and R. M. Holmes, The Structural Arrangement and Relative Abundance of Aliphatic Units May Effect Long-Wave Absorbance of Natural Organic Matter as Revealed by 1H NMR Spectroscopy, *Environ. Sci. Technol.*, 2018, **52**(21), 12526–12537.

14 N. Hertkorn, M. Harir, B. P. Koch, B. Michalke and P. Schmitt-Kopplin, High-Field NMR Spectroscopy and FTICR Mass Spectrometry: Powerful Discovery Tools for the Molecular Level Characterization of Marine Dissolved Organic Matter, *Biogeosciences*, 2013, **10**(3), 1583–1624.

15 N. G. A. Bell, A. A. L. Michalchuk, J. W. T. Blackburn, M. C. Graham and D. Uhrín, Isotope-Filtered 4D NMR Spectroscopy for Structure Determination of Humic Substances, *Angew. Chem., Int. Ed. Engl.*, 2015, **54**(29), 8382–8385.

16 N. Hertkorn, C. Ruecker, M. Meringer, R. Gugisch, M. Frommberger, E. M. Perdue, M. Witt and P. Schmitt-Kopplin, High-Precision Frequency Measurements: Indispensable Tools at the Core of the Molecular-Level Analysis of Complex Systems, *Anal. Bioanal. Chem.*, 2007, **389**(5), 1311–1327.
17 A. G. Marshall, C. L. Hendrickson and G. S. Jackson, Fourier Transform Ion Cyclotron Resonance Mass Spectrometry: A Primer, *Mass Spectrom. Rev.*, 1998, **17**(1), 1–35.
18 S. Kim, R. W. Kramer and P. G. Hatcher, Graphical Method for Analysis of Ultrahigh-Resolution Broadband Mass Spectra of Natural Organic Matter, the van Krevelen Diagram, *Anal. Chem.*, 2003, **75**(20), 5336–5344.
19 E. B. Kujawinski and M. D. Behn, Automated Analysis of Electrospray Ionization Fourier Transform Ion Cyclotron Resonance Mass Spectra of Natural Organic Matter, *Anal. Chem.*, 2006, **78**(13), 4363–4373.
20 W. C. Hockaday, J. M. Purcell, A. G. Marshall, J. A. Baldock and P. G. Hatcher, Electrospray and Photoionization Mass Spectrometry for the Characterization of Organic Matter in Natural Waters: A Qualitative Assessment, *Limnol. Oceanogr.*, 2009, **7**, 81–95.
21 R. L. Sleighter and P. G. Hatcher, *Fourier Transform Mass Spectrometry for the Molecular Level Characterization of Natural Organic Matter: Instrument Capabilities, Applications, and Limitations*, INTECH Open Access Publisher, 2011.
22 N. Hertkorn, M. Frommberger, M. Witt, B. P. Koch, P. Schmitt-Kopplin and E. M. Perdue, Natural Organic Matter and the Event Horizon of Mass Spectrometry, *Anal. Chem.*, 2008, **80**(23), 8908–8919.
23 T. Solouki, M. A. Freitas and A. Alomary, Gas-Phase Hydrogen/Deuterium Exchange Reactions of Fulvic Acids: An Electrospray Ionization Fourier Transform Ion Cyclotron Resonance Mass Spectral Study, *Anal. Chem.*, 1999, **71**(20), 4719–4726.
24 Y. Kostyukevich, A. Kononikhin, I. Popov and E. Nikolaev, Simple Atmospheric Hydrogen/Deuterium Exchange Method for Enumeration of Labile Hydrogens by Electrospray Ionization Mass Spectrometry, *Anal. Chem.*, 2013, **85**(11), 5330–5334.
25 A. C. Stenson, B. M. Ruddy and B. J. Bythell, Ion Molecule Reaction H/D Exchange as a Probe for Isomeric Fractionation in Chromatographically Separated Natural Organic Matter, *Int. J. Mass Spectrom.*, 2014, **360**, 45–53.
26 Y. Kostyukevich, A. Kononikhin, I. Popov, O. Kharybin, I. Perminova, A. Konstantinov and E. Nikolaev, Enumeration of Labile Hydrogens in Natural Organic Matter by Use of Hydrogen/Deuterium Exchange Fourier Transform Ion Cyclotron Resonance Mass Spectrometry, *Anal. Chem.*, 2013, **85**(22), 11007–11013.
27 Y. Kostyukevich, T. Acter, A. Zherebker, A. Ahmed, S. Kim and E. Nikolaev, Hydrogen/Deuterium Exchange in Mass Spectrometry, *Mass Spectrom. Rev.*, 2018, **37**, 811–853.
28 A. Zherebker, Y. Kostyukevich, A. Kononikhin, V. A. Roznyatovsky, I. Popov, Y. K. Grishin, I. V. Perminova and E. Nikolaev, High Desolvation Temperature Facilitates the ESI-Source H/D Exchange at Non-Labile Sites of Hydroxybenzoic Acids and Aromatic Amino Acids, *Analyst*, 2016, **141**(8), 2426–2434.

29 A. Zherebker, Y. Kostyukevich, A. Kononikhin, O. Kharybin, A. I. Konstantinov, K. V. Zaitsev, E. Nikolaev and I. V. Perminova, Enumeration of Carboxyl Groups Carried on Individual Components of Humic Systems Using Deuteromethylation and Fourier Transform Mass Spectrometry, *Anal. Bioanal. Chem.*, 2017, 1–12.

30 J. Atzrodt, V. Derdau, T. Fey and J. Zimmermann, The Renaissance of H/D Exchange, *Angew. Chem., Int. Ed. Engl.*, 2007, **46**(41), 7744–7765.

31 A. Y. Zherebker, D. Airapetyan, A. I. Konstantinov, Y. I. Kostyukevich, A. S. Kononikhin, I. A. Popov, K. V. Zaitsev, E. N. Nikolaev and I. V. Perminova, Synthesis of Model Humic Substances: A Mechanistic Study Using Controllable H/D Exchange and Fourier Transform Ion Cyclotron Resonance Mass Spectrometry, *Analyst*, 2015, **140**(13), 4708–4719.

32 T. Dittmar, B. Koch, N. Hertkorn and G. Kattner, A Simple and Efficient Method for the Solid-Phase Extraction of Dissolved Organic Matter (SPE-DOM) from Seawater, *Limnol. Oceanogr.: Methods*, 2008, **6**, 230–235.

33 Y. I. Kostyukevich, G. N. Vladimirov and E. N. Nikolaev, Dynamically Harmonized FT-ICR Cell with Specially Shaped Electrodes for Compensation of Inhomogeneity of the Magnetic Field. Computer Simulations of the Electric Field and Ion Motion Dynamics, *J. Am. Soc. Mass Spectrom.*, 2012, **23**(12), 2198–2207.

34 A. Zherebker, A. V. Turkova, Y. Kostyukevich, A. Kononikhin, K. V. Zaitsev, I. A. Popov, E. Nikolaev and I. V. Perminova, Synthesis of Carboxylated Styrene Polymer for Internal Calibration of Fourier Transform Ion Cyclotron Resonance Mass-Spectrometry of Humic Substances, *Eur. J. Mass Spectrom.*, 2017, **23**(4), 156–161.

35 R. L. Sleighter, G. A. McKee, Z. Liu and P. G. Hatcher, Naturally Present Fatty Acids as Internal Calibrants for Fourier Transform Mass Spectra of Dissolved Organic Matter, *Limnol. Oceanogr.: Methods*, 2008, **6**(6), 246–253.

36 E. V. Kunenkov, A. S. Kononikhin, I. V. Perminova, N. Hertkorn, A. Gaspar, P. Schmitt-Kopplin, I. A. Popov, A. V. Garmash and E. N. Nikolaev, Total Mass Difference Statistics Algorithm: A New Approach to Identification of High-Mass Building Blocks in Electrospray Ionization Fourier Transform Ion Cyclotron Mass Spectrometry Data of Natural Organic Matter, *Anal. Chem.*, 2009, **81**(24), 10106–10115.

37 B. P. Koch, T. Dittmar, M. Witt and G. Kattner, Fundamentals of Molecular Formula Assignment to Ultrahigh Resolution Mass Data of Natural Organic Matter, *Anal. Chem.*, 2007, **79**(4), 1758–1763.

38 B. P. Koch and T. Dittmar, From Mass to Structure: An Aromaticity Index for High-Resolution Mass Data of Natural Organic Matter, *Rapid Commun. Mass Spectrom.*, 2006, **20**(5), 926–932.

39 Y. Kostyukevich, A. Kononikhin, A. Zherebker, I. Popov, I. Perminova and E. Nikolaev, Enumeration of Non-Labile Oxygen Atoms in Dissolved Organic Matter by Use of $^{16}O/^{18}O$ Exchange and Fourier Transform Ion-Cyclotron Resonance Mass Spectrometry, *Anal. Bioanal. Chem.*, 2014, **406**(26), 6655–6664.

40 R. L. Sleighter, Z. Liu, J. Xue and P. G. Hatcher, Multivariate Statistical Approaches for the Characterization of Dissolved Organic Matter Analyzed by Ultrahigh Resolution Mass Spectrometry, *Environ. Sci. Technol.*, 2010, **44**(19), 7576–7582.

41 P. G. Hatcher and J. L. Faulon, Coalification of Lignin to Form Vitrinite: A New Structural Template Based on an Helical Structure, *J. Am. Chem. Soc.*, 1994, **39**, 7–12.

42 A. Y. Zherebker, Y. I. Kostyukevich, A. S. Kononikhin, E. N. Nikolaev and I. V. Perminova, Molecular Compositions of Humic Acids Extracted from Leonardite and Lignite as Determined by Fourier Transform Ion Cyclotron Resonance Mass Spectrometry, *Mendeleev Commun.*, 2016, **26**(5), 446–448.

43 P. G. Hatcher and D. J. Clifford, The Organic Geochemistry of Coal: From Plant Materials to Coal, *Org. Geochem.*, 1997, **27**, 251–257.

44 V. A. Krassilov, Coal-Bearing Deposits of the Soviet Far East, *Geol. Soc. Am., Spec. Pap.*, 1992, **267**, 263–267.

45 J. Dehmer, Petrographical and Organic Geochemical Investigation of the Oberpfalz Brown Coal Deposit, *Int. J. Coal Geol.*, 1989, **11**(3-4), 273–290.

46 N. H. Werstiuk and G. Timmins, Protium-Deuterium Exchange of Alkylated Benzenes in Dilute Acid at Elevated Temperatures, *Can. J. Chem.*, 1989, **67**(11), 1744–1747.

47 M. Guttman, D. D. Weis, J. R. Engen and K. K. Lee, Analysis of Overlapped and Noisy Hydrogen/Deuterium Exchange Mass Spectra, *J. Am. Soc. Mass Spectrom.*, 2013, **24**(12), 1906–1912.

48 S. M. Shevchenko and G. W. Bailey, The Mystery of the Lignin-Carbohydrate Complex: A Computational Approach, *J. Mol. Struct.*, 1996, **364**(2), 197–208.

49 G. Brunow, I. Kilpelainen, J. Sipila, K. Syrjanen, P. Karhunen, H. Setala and P. Rummakko, Oxidative Coupling of Phenols and the Biosynthesis of Lignin, *J. Am. Chem. Soc.*, 1998, 131–147.

50 W. Flaig and J. C. Salfeld, Nachweis Der Bildung von Hydroxy-*p*-Benzochinon Als Zwischenprodukt Bei Der Autoxydation von Hydrochinon in Schwach Alkalischer L{ö}sung, *Naturwissenschaften*, 1960, **47**(22), 516.

51 R. L. Sleighter and P. G. Hatcher, The Application of Electrospray Ionization Coupled to Ultrahigh Resolution Mass Spectrometry for the Molecular Characterization of Natural Organic Matter, *J. Mass Spectrom.*, 2007, **42**(5), 559–574.

52 A. J. Simpson, D. J. McNally and M. J. Simpson, NMR Spectroscopy in Environmental Research: From Molecular Interactions to Global Processes, *Prog. Nucl. Magn. Reson. Spectrosc.*, 2011, **3**(58), 97–175.

53 P. Delahaye and M. Verzele, Analysis of Gallic, Digallic and Trigallic Acids in Tannic Acids by High-Performance Liquid Chromatography, *J. Chromatogr. A*, 1983, **265**, 363–367.

54 J. V. Castell, L. A. Martinez, M. A. Miranda and P. A. Tárrega, General Procedure for Isotopic (Deuterium) Labelling of Non-Steroidal Antiinflammatory 2-Arylpropionic Acids, *J. Labelled Compd. Radiopharm.*, 1994, **34**(1), 93–100.

55 R. K. Hill, C. Abächerli and S. Hagishita, Synthesis of (2*S*, 4*S*)-and (2*S*, 4*R*)-[5,5,5-$^{2}H_{3}$] Leucine from (*R*)-Pulegone, *Can. J. Chem.*, 1994, **72**(1), 110–113.

56 A. Zherebker, E. Shirshin, O. Kharybin, Y. Kostyukevich, A. Kononikhin, A. I. Konstantinov, D. Volkov, V. A. Roznyatovsky, Y. K. Grishin, I. V. Perminova, *et al.* Separation of Benzoic and Unconjugated Acidic Components of Leonardite Humic Material Using Sequential Solid-Phase Extraction at Different PH Values as Revealed by Fourier Transform Ion

Cyclotron Resonance Mass Spectrometry and Correlation Nuclear Magneti, *J. Agric. Food Chem.*, 2018, **66**(46), 12179–12187.

57 N. DiDonato and P. G. Hatcher, Alicyclic Carboxylic Acids in Soil Humic Acid as Detected with Ultrahigh Resolution Mass Spectrometry and Multi-Dimensional NMR, *Org. Geochem.*, 2017, **112**, 33–46.

58 E. I. Fedoros, A. A. Orlov, A. Zherebker, E. A. Gubareva, M. A. Maydin, A. I. Konstantinov, K. A. Krasnov, R. N. Karapetian, E. I. Izotova, S. E. Pigarev, *et al.* Novel Water-Soluble Lignin Derivative BP-C*x*−1: Identification of Components and Screening of Potential Targets *in Silico* and *in Vitro*, *OncoTargets Ther.*, 2018, **9**(26), 18578.

59 M. Marcotullio, A. Pelosi and M. Curini, Hinokinin, an Emerging Bioactive Lignan, *Molecules*, 2014, **19**(9), 14862–14878.

60 P. G. Hatcher, H. E. Lerch and T. V. Verheyen, Organic Geochemical Studies of the Transformation of Gymnospermous Xylem during Peatification and Coalification to Subbituminous Coal, *Int. J. Coal Geol.*, 1990, **16**(1), 193–196.

